Impact of cavity symmetry on mode suppression and increase of free spectral range in solid-state dye microlaser

Sergei Popov[1], Sebastien Ricciardi[1], Ari T. Friberg[1,3,4], and Sergey Sergeyev[2]

[1] *Royal Institute of Technology, Kista 16440, Sweden*
[2] *Waterford Institute of Technology, Waterford, Ireland*
[3] *Helsinki University of Technology, 02015 Espoo, Finland*
[4] *University of Joensuu, 80101 Joensuu, Finland*

Received August 16, 2007

We describe modeling the solid-state dye laser with the microcavity size comparable to light wavelength. Certain symmetry in the allocation of gain material leads to depletion of odd longitudinal modes that, in turn, increases the tunability range of the microlaser. We provide simple physical explanation for the modeling results.

OCIS codes: 140.2050, 140.3600, 160.5470.

Micro-scaled lasers are becoming enabling components for explosively developing nano-sciences and bio-applications. Numerous tasks in sensing and monitoring techniques, such as drug screening, massive testing of biological specimens, or implementation of 'lab-on-a-chip' systems, require the use of tunable coherent light sources[1−3]. For most of them, dye lasers can be efficient "problem solvers" owing to their favorable features: high brightness and coherence, narrow radiation linewidth, and broadband wavelength tunability in the visible part of the electromagnetic spectrum[4].

Recently, new advances were reported in the realization of micro-structured dye lasers[5−7]. In particular, the operation of micro-fluidic dye lasers with the cavity size in the millimeter range or slightly smaller was demonstrated. However, the use of a liquid gain medium can limit further down-sizing of such microcavities to be implemented in high-density integrated photonic devices.

In this report, we describe the modeling of solid-state dye lasers with a microcavity of a typical scale required for micro-(nano-)photonics applications, $4-10$ μm. The renewed interest to solid-state polymer-dye compositions as lasing media for micro- and nano-photonics applications is based on recent progress in polymer physics and considerable improvements of dye properties — first of all, stability against photo-bleaching and aggregation at high concentrations[8−10]. As the gain material, we consider a solid solution of Rh6G dye embedded in a PMMA polymer host matrix. Finite element method (FEM) implemented in Comsol Multiphysics package is used for the simulation. Comparing the numerical results for different positions of excitation sources within the microcavity, we observe significant depletion of the odd longitudinal modes and enhancement of the even laser modes.

Our simulation is based on the model of a liquid dye microcavity laser demonstrated recently[11]. Since the subject of our investigation is a solid-state dye laser with the cavity size comparable to the operation wavelength, we needed to make appropriate changes of the design. First, we substitute the microfluidic channel (containing a liquid dye solution and placed between the two triangle-shaped sections of the coupled microcavity) with a solid polymer bar embedded with dye molecules. A large number of dye molecules (500 is a reasonable value for rather homogeneous distribution in the gain section) as point excitation sources randomly allocated inside the polymer bar are used to simulate gain medium. Here we use a multi-point excitation (MPE) source instead of a single-point excitation (SPE) close to the edge of the cavity as in Ref. [11] (point A in Fig. 1). Such an approach describes better a real physical situation. Secondly, we have decreased the size of the microcavity to the light wavelength scale. The microlaser layout is similar to that studied in Ref. [1] (see Fig. 1): two triangular half-cavity parts, the central gain slab, and an output coupling prism. We assign typical values for the refractive indices of the various parts, i.e., $n_{\mathrm{d-p}} = 1.43$ for the dye-polymer gain section and $n_{\mathrm{pol}} = 1.6$ for the polymer (SU-8) parts of the microcavity, but we do not specify the dispersion of the gain medium. This is quite reasonable, since we consider only a relatively small wavelength bandwidth of $455-600$ nm corresponding to real dye lasers. Both absorption and amplification in the gain material are also ignored to keep the model as simple as possible.

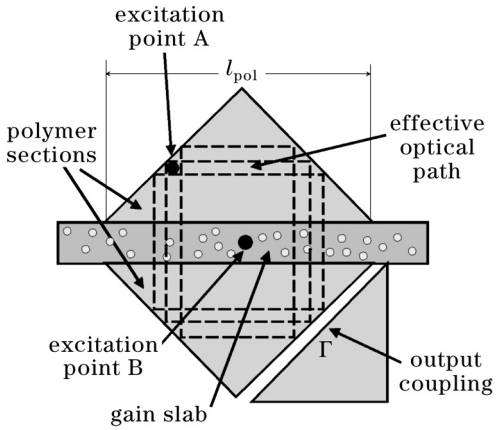

Fig. 1. Microcavity of solid-state dye laser, illustrating the optical paths of the effective cavity modes (dashed lines) and the polymeric gain material that contains dye molecules (hollow dots in the central slab).

A planar microcavity topology with pumping through the top facet allows employing two-dimensional (2D) model for transverse-electric (TE) waves, where the electric field vector only has a component perpendicular to the plane cavity. To obtain the intensity spectrum of the microcavity modes, we find solutions for Helmholtz equation inside the cavity and perform integration of the output power along the out-coupling boundary Γ (Fig. 1). Dye molecules, represented as point sources of spherical waves (hollow dots in Fig. 1), simulate excitation field inside the gain slab. The resonance modes are found within the region of the dye luminescence, between 500 and 660 THz ($455-600$ nm). For the demonstration and discussion of the results, it is more convenient to represent the microcavity spectra as a function of mode numbers rather than frequencies. We apply relations similar to those in Ref. [11] and phase matching conditions for round-trip mode path to calculate mode spacing and numbers:

$$m = \frac{1}{2\,\pi}\left(\nu_m L_{\rm eff}\frac{2\,\pi}{c} + \varphi\right), \tag{1}$$

where we consider m rounded to the nearest positive integer (mode number), ν_m is the resonance frequency, φ is the phase change due to the reflections at the microcavity walls (from the Fresnel coefficients for the amplitude of the electric field)[11,12], and $L_{\rm eff}$ is the effective optical path constructed as

$$L_{\rm eff} = 2(n_{\rm d-p} l_{\rm d-p} + n_{\rm pol} l_{\rm pol}), \tag{2}$$

where $n_{\rm d-p}$ and $n_{\rm pol}$ are the refractive indices of the dye-polymer gain slab and polymer half-cavities, whereas $l_{\rm d-p}$ and $l_{\rm pol}$ are the thicknesses of the dye-polymer slab and the length of the polymer triangle side adjacent to the dye-polymer slab, respectively (Fig. 1). The output coupling of the radiating modes occurs through an air gap $l_{\rm air}$ at the boundary Γ by means of catching the evanescent field outside the cavity. Using the value $l_{\rm pol} = 4$ μm, whereas $l_{\rm d-p}$ is kept at about 20% of $l_{\rm pol}$ and $l_{\rm air}$ at 3% of $l_{\rm pol}$, we obtain effective optical paths for the modes as long as $L_{\rm eff} \sim 15$ μm.

The main result of the simulations is shown in Fig. 2, where we compare the resonance spectra of the longitudinal modes as functions of the mode numbers for two models: one is for our modified MPE design and the other is for the SPE scheme considered in Ref. [11]. For the microcavity dye laser with the MPE source (hollow dots in the central slab in Fig. 1), we obtain noticeable physical features not observed in the original SPE model: odd longitudinal modes are significantly depleted, while the even modes are strongly enhanced (Fig. 2). Figure 2 displays the total power of the electric field integrated along the out-coupling boundary Γ. For a proper comparison, the results are normalized, i.e., the values for the MPE arrangement are divided by 500, the number of SPE sources. Thus, the total pump power is the same as for the SPE design and it is evenly distributed among 500 point sources randomly allocated in the polymer-dye slab.

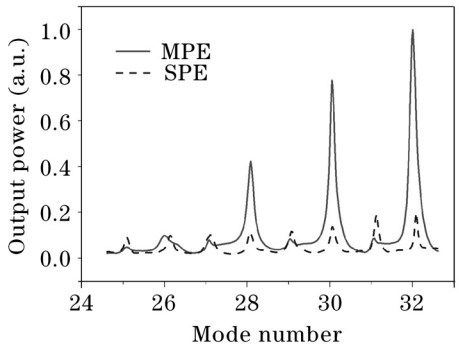

Fig. 2. Microcavity mode spectra for different excitation schemes: single-point at the edge of the cavity and multi-point inside the central gain slab. The output power is normalized by the number of excitation points.

The longitudinal mode numbers inside a microsized cavity should not be interpreted simply as the numbers of nodes and antinodes of one standing wave, like in the case of one-dimensional (1D) long laser cavity. However, here it is possible and instructive to consider that the mode numbers refer to the effective optical path length in the central region of the cavity, since the parity of these numbers can help to explain the relation between the mode properties shown in Fig. 2, the microcavity symmetry, and the allocation of the excitation sources.

Standing waves building up the cavity modes should satisfy the phase-matching conditions for wave round trips along the closed optical path. The microcavity with the inserted gain section between the two parts (not considering the output coupling prism) possesses spatial symmetry about the horizontal axis through the central slab. The position of the excitation source(s) relative to this axis and the mode parity (treated as the parity of the mode number) play an important role on how efficiently the pump energy is coupled into the cavity modes.

To clarify this relationship, we consider the mode spectra for two different positions of the SPE sources placed far from and close to the horizontal symmetry axis,

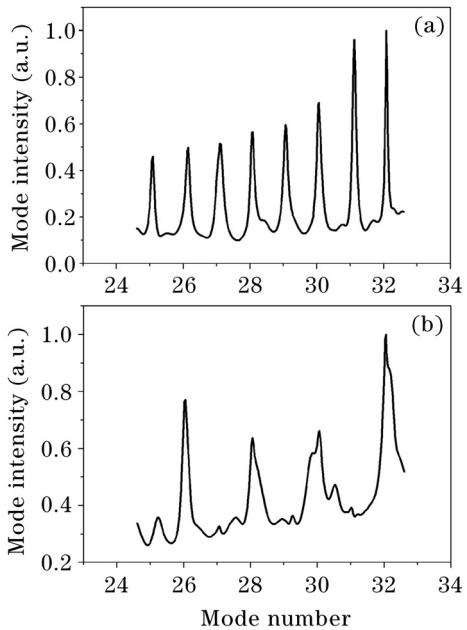

Fig. 3. Microcavity mode spectra for SPE sources allocated (a) at the edge (point A in Fig. 1) and (b) in the center (point B in Fig. 1) of the microcavity.

i.e., points A and B in Fig. 1, respectively. The corresponding mode spectra are illustrated in Fig. 3. The graphs show that for central point B the intensities of the modes with odd mode number are considerably suppressed (Fig. 3(b)), whereas the spectrum for edge point A does not exhibit any such dependence on the mode number parity (Fig. 3(a)). We can reasonably explain this phenomenon with different coupling efficiencies of the SPE pumping wave into the cavity modes with odd and even numbers using the mutual symmetry between the cavity modes and the location of the excitation source.

When the excitation source, point A in Fig. 4(a), is placed close to the cavity edge, the phase fronts of the spherical wave (solid line) cross the mode path (dashed line) at points which in all likelihood have different phases for the even and the odd numbered modes, for example, pairs 1-2 and 3-4. Although, by symmetry, the even numbered modes would have the same phase at point pairs 1-1′ and 3-3′, the phase of the excitation wave would not match. In such a case, therefore, no favorable conditions are created for the coupling of the pump excitation into the modes with different parities. The result then is a fairly even distribution of the output intensity among the odd and even modes (Fig. 3(a)).

Next, we consider the excitation source, point B in Fig. 4(b), at the center of the cavity. For the even numbered resonance modes, the symmetrical cavity geometry leads to the same phase of the optical wave (dashed line) at every pair of points placed symmetrically at equal distances above and below the horizontal axis, for example, point pairs 1-2 and 3-4. Since the SPE source emits a spherical wave (solid line), such a circumstance ensures an efficient transfer of the excitation energy into the cavity mode at these points due to constructive superposition. For the same working conditions, the odd numbered modes do not provide similar phase matching between the cavity modes and the spherical excitation waves, since the phases of the mode wave at point pairs 1-2 and 3-4 are no longer equal. Thus, the efficiency of the excitation coupling into the odd numbered modes is weaker (Fig. 3(b)). The large number of the points constituting the MPE source in the central section of the microcavity amplifies (and averages) the SPE effects. This is clearly seen from comparison between Figs. 2 and 3(b), where the residual ripples around odd modes in Fig. 3(a) (excited by the SPE source) are smoothed out after averaging over multiple sources.

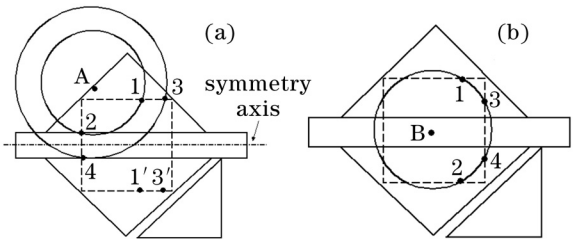

Fig. 4. Schematic representations of the overlapping between the excitation spherical wave (solid circle) and the microcavity modes (dashed square). (a) The source is placed at the cavity edge (point A in Fig. 1); (b) the source is placed in the cavity center (point B in Fig. 1).

In this paper, we have considered modeling a solid-state dye microlaser. The design, when the gain material is simulated as a multi-point excitation source placed between the two similar parts of the cavity, demonstrates the depletion of odd modes and the increased output radiation in even laser modes. We attribute this effect to the symmetry relation between the cavity shape and allocation of the excitation sources (the gain section) within the cavity. The mode suppression effect can be used to tailor the tunability of microcavity lasers, since it increases the free spectral range while keeping the same cavity size. Besides the factors based on geometry, a particular composition and distribution of the polymer-dye gain material can influence the mode depletion behavior. This effect requires more accurate simulations, including modeling inhomogenous radiation patterns for dye molecules and amplification of the optical wave.

S. Popov, S. Ricciardi, and A. T. Friberg (with Royal Institute of Technology) acknowledge financial support from the Swedish Foundation for Strategic Research (SSF). S. Popov's e-mail address is sergeip@kth.se.

References

1. I. M. White, H. Zhu, J. D. Suter, N. M. Hanumegowda, H. Oveys, M. Zourob, and X. Fan, IEEE Sensors J. **7,** 28 (2007).
2. H. Craighead, Nature **442,** 387 (2006).
3. D. Psaltis, S. R. Quake, and C. Yang, Nature **442,** 381 (2006).
4. F. J. Duarte, (ed.) *Tunable Lasers Handbook* (Elsevier, Amsterdam, 1995).
5. S. Balslev and A. Kristensen, Opt. Express **13,** 344 (2005).
6. B. Bilenberg, T. Rasmussen, S. Balslev, and A. Kristensen, J. Appl. Phys. **99,** 023102 (2006).
7. Y. Cheng, K. Sugioka, and K. Midorikawa, Opt. Lett. **29,** 2007 (2004).
8. A. Costela, I. García-Moreno, D. del Agua, O. García, and R. Sastre, Appl. Phys. Lett. **85,** 2160 (2004).
9. F. Duarte and R. O. James, Opt. Lett. **28,** 2088 (2003).
10. A. Costela, I. García-Moreno, C. Gómez, O. García, and R. Sastre, Appl. Phys. B **75,** 827 (2002).
11. M. Hansen-Gersborg, S. Balslev, and N. A. Mortensen, J. Opt. A **8,** 17 (2006).
12. E. Hecht, *Optics* (4th edn.) (Addison Wesley, New York, 2002).